

RESEARCH ARTICLE | AUGUST 05 2016

# Compact electret energy harvester with high power output



P. Pondrom; G. M. Sessler; J. Bös; T. Melz



*Appl. Phys. Lett.* 109, 053906 (2016)

<https://doi.org/10.1063/1.4960480>



## Articles You May Be Interested In

Electret transducer for vibration-based energy harvesting

*Appl. Phys. Lett.* (May 2015)

Vibration-based energy harvesting with piezoelectrets having high  $d_{31}$  activity

*Appl. Phys. Lett.* (May 2016)

Energy harvesting from vibration with cross-linked polypropylene piezoelectrets

*AIP Advances* (July 2015)

06 November 2024 14:31:28



Applied Physics Letters

# Special Topics Open for Submissions

[Learn More](#)

This article may be downloaded for personal use only. Any other use requires prior permission of the author and AIP Publishing. This article appeared in 'P. Pondrom, G. M. Sessler, J. Bös, T. Melz; Compact electret energy harvester with high power output. *Appl. Phys. Lett.* 1 August 2016; 109 (5): 053906' and may be found at <https://doi.org/10.1063/1.4960480>

## Compact electret energy harvester with high power output

P. Pondrom,<sup>1,2,a)</sup> G. M. Sessler,<sup>1</sup> J. Bös,<sup>2</sup> and T. Melz<sup>2</sup>

<sup>1</sup>Institute for Telecommunications Technology, Technische Universität Darmstadt, Merckstr. 25, 64283 Darmstadt, Germany

<sup>2</sup>System Reliability and Machine Acoustics SzM, Technische Universität Darmstadt, Magdalenenstr. 4, 64289 Darmstadt, Germany

(Received 29 February 2016; accepted 25 July 2016; published online 5 August 2016)

Compact electret energy harvesters, based on a design recently introduced, are presented. Using electret surface potentials in the 400 V regime and a seismic mass of 10 g, it was possible to generate output power up to 0.6 mW at 36 Hz for an input acceleration of 1 g. Following the presentation of an analytical model allowing for the calculation of the power generated in a load resistance at the resonance frequency of the harvesters, experimental results are shown and compared to theoretical predictions. Finally, the performance of the electret harvesters is assessed using a figure of merit. Published by AIP Publishing. [<http://dx.doi.org/10.1063/1.4960480>]

Energy harvesting is defined as the conversion of energy from environmental sources into electrical energy that can be stored and used to power electrical circuits such as wireless sensor nodes.<sup>1,2</sup> Unlike classical battery-equipped systems, energy harvesters do not require external charging or battery replacement, which is advantageous for applications where electrical circuits are placed in remote locations. Typical environmental sources for energy harvesting are light, electromagnetic waves, thermal gradients, or mechanical vibrations. Energy from mechanical vibrations may be converted into electrical energy using electromagnetic, piezoelectric, or electrostatic transduction.

Piezoelectret<sup>3–7</sup> and electret energy harvesters<sup>8–10</sup> are a particular kind of electrostatic harvesters. These basically consist of an electrically polarized capacitor whose capacitance is modulated in response to input vibrations. This modulation is either a change of the overlapping area of the electrodes with constant air gap thickness (“in-plane” type)<sup>11–19</sup> or a variation of the air gap thickness with constant overlapping area (“out-of-plane” type).<sup>11,12,20–23</sup> In the case of electret energy harvesters, the polarization voltage is generated by an electret film placed between the capacitor electrodes, eliminating the need for an external voltage in the regime of a few hundred volts. These harvesters are most frequently based on Micro-Electro-Mechanical System (MEMS) technology.<sup>14–19,21–23</sup> More recently, electret biasing has also been suggested to replace the external polarization of dielectric elastomer generators.<sup>24,25</sup>

The electret energy harvesters investigated in this study are of the out-of-plane type. Their simple design is based on electret harvesters presented previously<sup>10</sup> with compressive cellular polypropylene (PP) spacers between electret and ground electrode. The goal of the present experiments was to lower the resonance frequency from values above 1 kHz to the range around 100 Hz or below, where conditions for vibration-based energy harvesting are much better.<sup>1</sup> It was also intended to increase the power output of the device, even for a reduced seismic mass. Both goals were to be

achieved with a modification of the compressive cellular spacers.

In the following, the design of the electret harvesters and the experimental setup are discussed, followed by an analytical model. Then experimental results for the charge sensitivity, damping ratio, and generated power of the harvesters are shown and compared with theoretical calculations. Finally, after an analysis of the results, conclusions are presented.

The experimental setup of the electret energy harvesters is shown in Fig. 1 and described in more detail in the supplementary material.<sup>26</sup> The harvesters consist of a fluoroethylene propylene (FEP) electret film metalized on one side and glued with its metalized side to a seismic mass made of brass. A ground electrode is separated from the electret by an air gap maintained by three or four small stacks made of cellular polypropylene (PP) films.<sup>26</sup> These stacks are inserted in holes of the ground electrode. Since the height of the stacks is larger than the thickness of the ground electrode, they stick out of the holes and thus govern the thickness of the air gap. The elastic properties of these stacks<sup>27</sup> determine largely the restoring force of the device and thus its resonance frequency. A plastic membrane fixed to the housing applies a static pressure on the seismic mass and prevents it from moving sideways. Its contribution to the restoring force is relatively small. The charge generated by the harvester in a load resistance  $R_l$  is measured using a charge amplifier that is in series with  $R_l$ .

The power  $P$  generated by an electret energy harvester in  $R_l$  in response to the input acceleration  $a$  at the circular frequency  $\omega$  is derived from the equation of motion of the harvester. In analogy to the power obtained from a piezoelectret harvester of similar design,<sup>6</sup> it can be written as<sup>10</sup>

$$\begin{aligned}
 P &= \frac{R_l \left( \frac{C_s \epsilon_r V_E}{\omega_0^2 (\epsilon_r t_A + t_E)} \omega a \right)^2}{\left[ \left( \frac{\omega^2}{\omega_0^2} - 1 \right)^2 + 4 \zeta^2 \left( \frac{\omega}{\omega_0} \right)^2 \right] [1 + (R_l C_s \omega)^2]} \\
 &= \frac{R_l}{1 + (R_l C_s \omega)^2} (q_0 \omega)^2, \quad (1)
 \end{aligned}$$

<sup>a)</sup>Electronic mail: pondromp@gmail.com

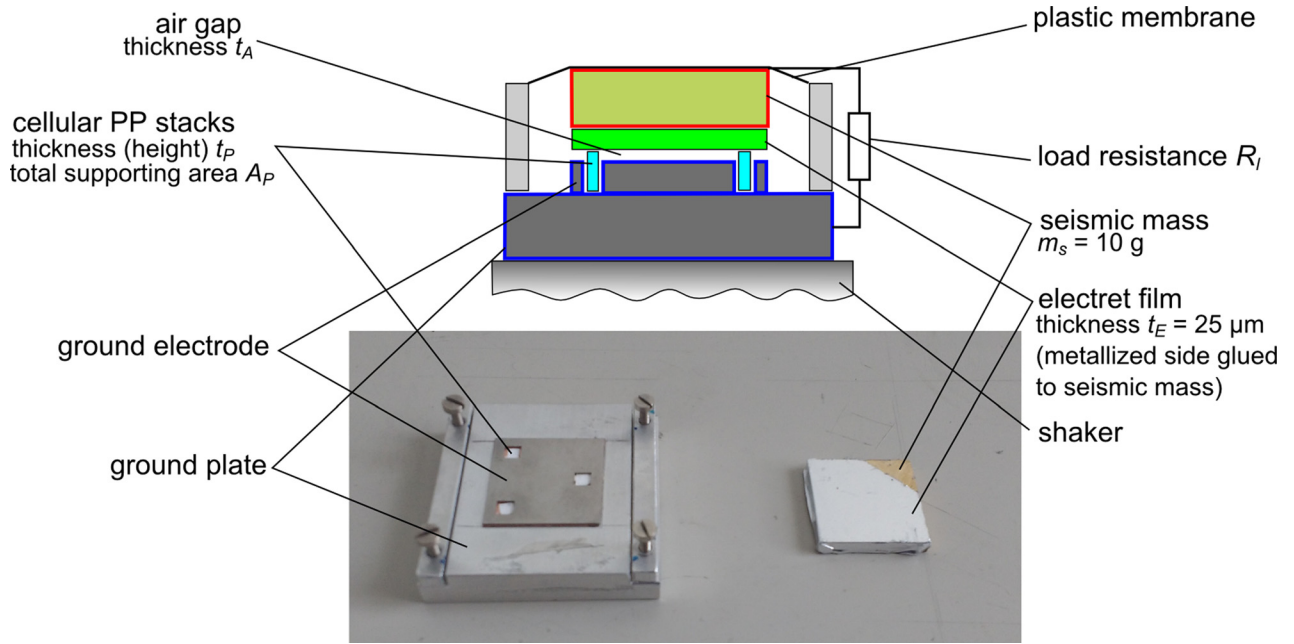


FIG. 1. Top: schematics of an electret energy harvester. Bottom: left: support (ground plate) with ground electrode. The cellular PP stacks are inserted in the holes of the ground electrode. Right: seismic mass with electret film glued on the surface.

where  $C_s$  is the harvester capacitance,  $\epsilon_r$  is the dielectric permittivity of FEP,  $V_E$  is the electret surface potential,  $t_A$  is the air gap thickness,  $t_E$  is the electret film thickness,  $\zeta = \Delta\omega/2\omega_0$  is the damping ratio corresponding to half the half-power bandwidth  $\Delta\omega/\omega_0$ , and  $q_0$  is the RMS value of the charge generated in short-circuit (see Ref. 10 for limitations of Eq. (1)). For energy harvesters with relatively weak electromechanical coupling coefficients ( $k^2 \ll 2\zeta$ ), the backward effect due to the electromechanical coupling can be neglected (see the supplementary material).<sup>26</sup> The natural frequency  $\omega_0$  may be expressed as

$$\omega_0 = \sqrt{\frac{1}{m_s c_m}} = \sqrt{\frac{Y A_P}{m_s t_P}}, \quad (2)$$

where  $m_s$  is the seismic mass,  $c_m$  is the mechanical compliance of the cellular polypropylene spacers,  $Y$  is their Young's modulus,  $t_P$  is their thickness, and  $A_P$  (different from the air gap area  $A_A$ ) is their cross sectional area which supports the seismic mass (see Fig. 1). The measured resonance frequency  $\omega_{res} = \omega_0 \sqrt{1 - \zeta^2}$  can significantly differ from  $\omega_0$  for high damping ratios.

With the optimal load resistance,

$$R_{opt} = 1/(C_s \omega_0), \quad (3)$$

the maximum power  $P_{opt}$  generated at  $\omega_0$  in response to  $a$  follows from Eq. (1) as

$$P_{opt} = \frac{a^2 C_s \epsilon_r^2 V_E^2}{\omega_0^3 (\epsilon_r t_A + t_E)^2 8 \zeta^2}. \quad (4)$$

Thus, since  $\omega_0$  can be decreased according to Eq. (2) through the reduction of  $A_P$  (in the range of  $30 \text{ mm}^2$  to  $3 \text{ mm}^2$ ) or the increase of  $t_P$  (in the range of  $50 \text{ μm}$ – $1 \text{ mm}$ ), it is not necessary to increase  $m_s$  to generate more power. This is a major advantage for the design of compact and

lightweight electret energy harvesters. However, one has to take into consideration that the deflection of the seismic mass increases with decreasing  $\omega_0$  and eventually reaches  $t_A$ . The limits thus imposed are discussed in the supplementary material.<sup>26</sup>

With piezoelectret harvesters, measurements were made with  $R_l = R_{opt}$  (Eq. (3)).<sup>5,6</sup> An alternative method is to calculate the maximum power from short-circuit charge measurements and  $R_{opt}$  as

$$P_{opt} = \frac{R_{opt} (q_0 \omega_0)^2}{1 + (R_{opt} C' \omega_0)^2} = \frac{\omega_0 q_0^2}{2 C_s}. \quad (5)$$

The main advantage of this method is its simplicity, since it does not require the use of a resistance precisely matching the stack impedance, but it necessitates an accurate measurement of the capacitance. In the following figures, the normalized power,<sup>28</sup>

$$P_N = P \left( \frac{g}{a} \right)^2, \quad (6)$$

generated by the energy harvesters, referred to an input acceleration of  $1 g$  ( $g = 9.81 \text{ m/s}^2$ ), is plotted.

Measurements of the normalized power generated by an electret harvester at a resonance frequency of  $540 \text{ Hz}$  in various load resistances are shown in Fig. 2, as well as a calculation based on Eq. (1), second part, with the measured value of  $q_0$ . The agreement between the power values calculated with Eq. (1) from  $q_0$  and those obtained from  $P = R_l I^2$ , where  $I$  is the measured current through  $R_l$ ,<sup>5,6</sup> is excellent and shows that calculations based on  $q_0$  are sufficient to characterize the performance of electret harvesters of known capacitance.

The charge sensitivity<sup>29</sup>  $9.81 q_0/a$  of several electret harvesters operating as accelerometers well below their resonance frequency is shown in Fig. 3 as a function of  $\omega_0$ . The

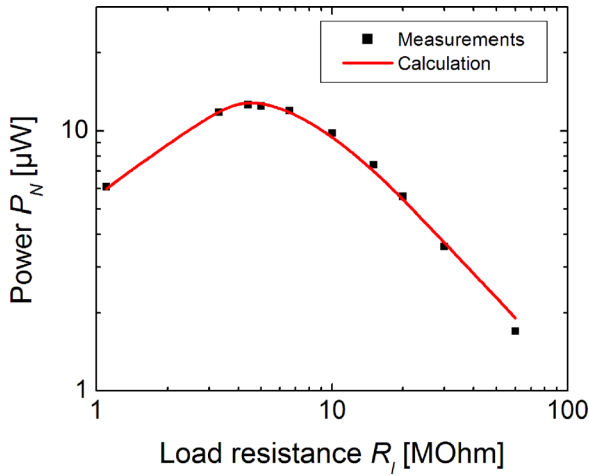


FIG. 2. Measurement of normalized power  $P_N$  generated by an electret energy harvester into various load resistances at a resonance frequency of 540 Hz. The harvester capacitance is 47 pF.

measured harvester capacitances show some scattering, reflecting varying air gap thicknesses. In order to take into account the effect of the capacitance on their performance, the harvesters are divided into two groups according to their capacitance. The variation of the resonance frequency in this and in the following figures is due to the use of the cellular PP stacks (see above) with diverse stiffnesses obtained by varying  $t_p$  and  $A_p$  (see the supplementary material).<sup>26</sup> As seen in Fig. 3, the sensitivity is proportional to  $1/\omega_0^2$ , as anticipated from Eq. (14) of Ref. 29. Compared to this earlier work,<sup>29,30</sup> the accelerometer sensitivity shows thus an improvement of almost a factor of 50 for similar seismic masses when the resonance frequency decreases from 2000 to 200 Hz. As expected, the accelerometers with greater capacitance (smaller air gap) are also more sensitive.

The measured damping ratios of the investigated energy harvesters as a function of their resonance frequencies are shown in Fig. 4 as well as a linear fit following a dependence on  $1/\omega_0$ . They were obtained by measuring the half-widths of the normalized powers in the harvester frequency

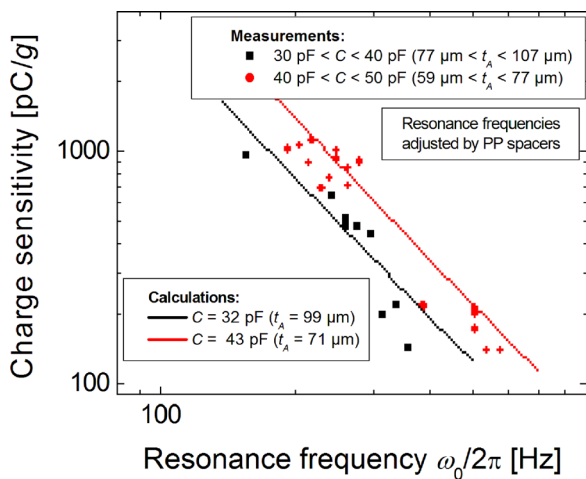


FIG. 3. Measured and calculated charge sensitivity of various energy harvesters used as accelerometers below their resonance frequency, as a function of their resonance frequency. The discrete values represent measured sensitivities and the full lines show the results calculated with Eq. (14) of Ref. 29.

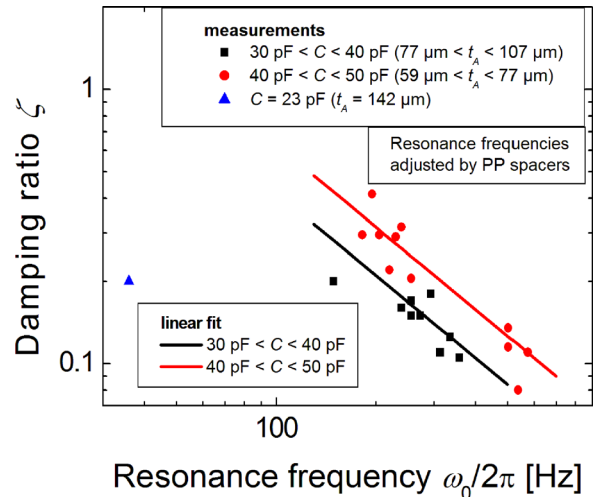


FIG. 4. Measured damping ratio  $\zeta$  and linear fit for various electret energy harvesters as a function of their resonance frequency. The solid lines are best fits assuming an inverse dependence of  $\zeta$  on  $\omega_0$ .

responses (see, for example, Fig. 6). The damping ratio  $\zeta$  can be expressed as

$$\zeta = \frac{D}{2\sqrt{m_s c_m}} = \frac{D}{2m_s \omega_0}, \quad (7)$$

where  $D$  is the damping coefficient of the energy harvester.<sup>31</sup> According to Eq. (3),  $P_{\text{opt}}$  is proportional to  $1/\zeta^2$ . Thus, it is desirable to minimize  $\zeta$  in order to maximize the amount of power generated at  $\omega_0$ . However, since mechanical vibrations often occur in a broader frequency range, energy harvesters should also have a large bandwidth (see below). The results presented in Fig. 4 show that the measured damping ratio  $\zeta$  decreases proportionally to  $1/\omega_0$ , which agrees with Eq. (7) if  $D$  is assumed to be frequency-independent. It also increases with increasing harvester capacitance (i.e., decreasing air gap thickness). This can be explained by greater viscous damping due to air streaming in thinner air gaps of the harvester.<sup>32</sup> Such damping can be reduced by drilling holes in the backplate of the harvester, which will shorten the path of air streaming in the air gap.

The normalized power  $P_N$  (see above) generated by the electret harvesters in  $R_{\text{opt}}$  at  $\omega_0$  is shown in Fig. 5. The

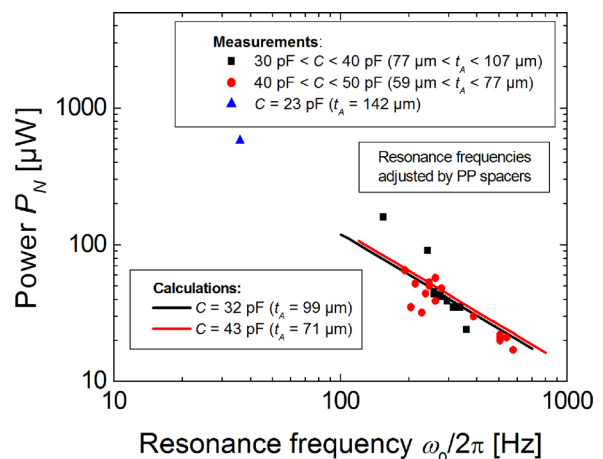


FIG. 5. Measured and calculated normalized power  $P_N$  generated by various electret energy harvesters as a function of  $\omega_0$ . For the calculations, the same parameter values are used as in Fig. 3.

TABLE I. Parameters used for the calculation of the power generated by the electret energy harvesters.

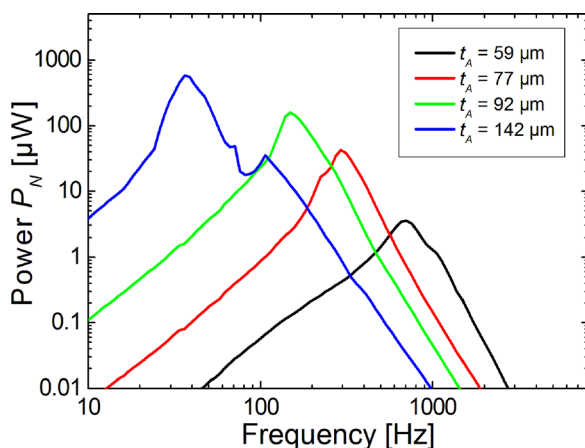
Parameter	$m_s$ [g]	$t_E$ [ $\mu\text{m}$ ]	$A_A$ [ $\text{cm}^2$ ]	$\epsilon_r$	$V_E$ [V]
Value	10	25	4	1.2	400

theoretical curves were calculated from Eq. (3) using the same parameters as for the sensitivities shown in Fig. 3 (see Table I) and the linear fits of the damping ratio shown in Fig. 4. The measured dependence on  $\omega_0$  agrees well with the calculations. The maximum power at resonance is only proportional to  $1/\omega_0$ , instead of  $1/\omega_0^3$  as predicted by Eq. (3). This difference is due to the dependence of  $\zeta$  on  $\omega_0$  (see Fig. 4) and the proportionality of  $P_{opt}$  to  $1/\zeta^2$ . Almost no increase of the power for smaller air gaps is noticed, which can also be explained by the greater damping due to air streaming through the smaller gap.

According to this dependence of  $P_{opt}$  on  $\omega_0$ , the generated power theoretically increases strongly towards low frequencies. However, since the deflection of the seismic mass is limited by the air gap thickness, the generated power is also limited. Larger seismic mass deflection requires increasing air gap thickness, but this results in decreasing electric field inside the air gap and thus in smaller harvester sensitivity (see Eq. (1)).

Finally, measured frequency responses of several electret energy harvesters are shown in Fig. 6. For all curves, the observed rise of the response below resonance is approximately proportional to  $\omega^2$  while the drop-off above resonance shows nearly a proportionality to  $1/\omega^4$ , as predicted by Eq. (1). The flexibility in the design of such harvesters allows for covering a frequency from well below 100 Hz to 1 kHz. The most sensitive harvesters have the lowest resonance frequency (see Eq. (3)), which is advantageous as most energy from mechanical vibrations is concentrated in this range. In particular, with a seismic mass of only 10 g it was possible to achieve a maximum normalized power of 0.6 mW at a resonance frequency of 36 Hz with a relative half-power bandwidth of 45%.

To assess the performance of the electret harvesters and compare them with previously reported harvesting devices

FIG. 6. Frequency response of normalized powers  $P_N$  generated by some electret energy harvesters.

as a function of their size and relative bandwidth  $\Delta\omega/\omega_0$ , the Bandwidth Figure of Merit ( $\text{FoM}_{\text{BW}}$ )<sup>1</sup> can be used. The  $\text{FoM}_{\text{BW}}$  of the electret harvesters with resonance frequencies of 70 Hz and 36 Hz is equal to 0.1%.

In this paper, compact energy harvesters based on a previous design<sup>10</sup> are presented. The circular polypropylene spacer rings were replaced with several polypropylene stacks to reduce the mechanical stiffness and, thus, the resonance frequency of the harvesters, and increase the generated power. Hence, it was possible to increase the normalized power by two orders of magnitude to 0.6 mW at a frequency of 36 Hz. It should be noticed, however, that the actual maximum achievable power is smaller than this, since the deflection of the seismic mass cannot exceed  $t_A$ . This is the case for<sup>26</sup> an acceleration of 0.25 g, corresponding to a power of 37  $\mu\text{W}$ . The backward coupling effect, expressed by the inclusion of  $k_{33}^2$ , was neglected in Eq. (1) since its contribution to the harvested power of the present harvesters is negligible. It should be noted, however, that by decreasing the resonance frequency below the above value or decreasing the air gap thickness,  $k_{33}^2$  must be included.<sup>26</sup>

Despite the harvesters' relatively simple design and low weight, the achieved maximum bandwidth figure of merit  $\text{FoM}_{\text{BW}}$  of 0.1% is considerably higher than those of  $d_{33}$ -based piezoelectret harvesters of similar design<sup>5,6</sup> and is comparable to that of  $d_{31}$ -based piezoelectret harvesters<sup>33</sup> and recent piezoelectric harvesters.<sup>34,35</sup> The present design can also be used in very sensitive accelerometers for low-frequency use. This opens an avenue to applications combining lightweight and very sensitive accelerometers and energy harvesters, for example, in structural health monitoring or medical instrumentation.

The authors are grateful to Dr. Joachim Hillenbrand for stimulating discussions during the initial phases of this work.

<sup>1</sup>P. D. Mitcheson, E. M. Yeatman, G. K. Rao, A. S. Holmes, and T. C. Green, *Proc. IEEE* **96**, 1457 (2008).

<sup>2</sup>E. Elvin and A. Erturk, *Advances in Energy Harvesting Methods* (Springer, New York, 2013).

<sup>3</sup>S. R. Anton and K. M. Farinholt, *Proc. SPIE* **8341**, 83410G (2012).

<sup>4</sup>S. R. Anton, K. M. Farinholt, and A. Erturk, *J. Int. Mater. Syst. Struct.* **25**, 1681 (2014).

<sup>5</sup>P. Pondrom, J. Hillenbrand, G. M. Sessler, J. Böös, and T. Melz, *Appl. Phys. Lett.* **104**, 172901 (2014).

<sup>6</sup>P. Pondrom, J. Hillenbrand, G. M. Sessler, J. Böös, and T. Melz, *IEEE Trans. Dielectr. Electr. Insul.* **22**, 1470 (2015).

<sup>7</sup>X. Zhang, L. Wu, and G. M. Sessler, *AIP Adv.* **5**, 077185 (2015).

<sup>8</sup>Y. Suzuki, *IEEJ Trans. Elec. Electron. Eng.* **6**, 101 (2011).

<sup>9</sup>S. Boisseau, G. Despesse, and A. Sylvestre, *Smart Mater. Struct.* **19**, 075015 (2010).

<sup>10</sup>J. Hillenbrand, P. Pondrom, and G. M. Sessler, *Appl. Phys. Lett.* **106**, 183902 (2015).

<sup>11</sup>S. Roundy, P. K. Wright, and J. Rabaey, *Comput. Commun.* **26**, 1131 (2003).

<sup>12</sup>S. P. Beeby, M. J. Tudor, and N. M. White, *Meas. Sci. Technol.* **17**, R175 (2006).

<sup>13</sup>O. D. Jefimenko and D. K. Walker, *IEEE Trans. Ind. Appl.* **IA-14**, 537 (1978).

<sup>14</sup>F. Peano and T. Tambosso, *J. Microelectromech. Syst.* **14**, 429 (2005).

<sup>15</sup>H.-W. Lo and Y.-C. Tai, *J. Microelectromech. Microeng.* **18**, 104006 (2008).

<sup>16</sup>Y. Naruse, N. Matsubara, K. Mabuchi, M. Izumi, and S. Suzuki, *J. Micromech. Microeng.* **19**, 094002 (2009).

- <sup>17</sup>Y. Suzuki, D. Miki, M. Edamoto, and M. Honzumi, *J. Micromech. Microeng.* **20**, 104002 (2010).
- <sup>18</sup>U. Bartsch, J. Gaspar, and O. Paul, *J. Micromech. Microeng.* **20**, 035016 (2010).
- <sup>19</sup>T. Masaki, K. Sakurai, T. Yokoyama, M. Ikuta, H. Sameshima, M. Doi, T. Seki, and M. Oba, *J. Micromech. Microeng.* **21**, 104004 (2011).
- <sup>20</sup>S. Boisseau, G. Despesse, T. Ricart, E. Defay, and A. Sylvestre, *Smart Mater. Struct.* **20**, 105013 (2011).
- <sup>21</sup>Y. Chiu and Y.-C. Lee, *J. Micromech. Microeng.* **23**, 015012 (2013).
- <sup>22</sup>T. Takahashi, M. Suzuki, T. Nishida, Y. Yoshikawa, and S. Aoyagi, in *Proceedings of the MEMS* (2015), p. 1145.
- <sup>23</sup>Q. Fu and Y. Suzuki, in *Proceedings of the Conference Solid-State Sensors Actuators Microsystems* (2015), p. 1925.
- <sup>24</sup>C. Jean-Mistral, T. Vu-Cong, and A. Sylvestre, *Smart Mater. Struct.* **22**, 104017 (2013).
- <sup>25</sup>D. Peter, R. Pichler, S. Bauer, and R. Schwödauer, *Extreme Mech. Lett.* **4**, 38 (2015).
- <sup>26</sup>See supplementary material at <http://dx.doi.org/10.1063/1.4960480> for detailed description of the experimental setup and discussion of backward electromechanical coupling and maximum power.
- <sup>27</sup>J. Hillenbrand, G. M. Sessler, and X. Zhang, *J. Appl. Phys.* **98**, 064105 (2005).
- <sup>28</sup>X. Zhang, G. M. Sessler, and Y. Wang, *J. Appl. Phys.* **116**, 074109 (2014).
- <sup>29</sup>J. Hillenbrand, S. Habertzettl, T. Motz, and G. M. Sessler, *J. Acoust. Soc. Am.* **129**, 3682 (2011).
- <sup>30</sup>J. Hillenbrand, T. Motz, and G. M. Sessler, *IEEE Sens. J.* **14**, 1770 (2014).
- <sup>31</sup>A. Erturk and D. J. Inman, *Smart Mater. Struct.* **17**, 065016 (2008).
- <sup>32</sup>Z. Skvor, *Acustica* **19**, 295 (1967/1968).
- <sup>33</sup>X. Zhang, P. Pondrom, L. Wu, and G. M. Sessler, *Appl. Phys. Lett.* **108**, 193903 (2016).
- <sup>34</sup>K. Ashraf, M. H. Khir, J. O. Dennis, and Z. Baharudin, *Sens. Actuators A* **195**, 123 (2013).
- <sup>35</sup>D. F. Berdy, P. Srisungsitthisunti, B. Jung, X. Xu, J. F. Rhoads, and D. Peroulis, *IEEE Trans. UFFC* **59**, 846 (2012).